

## FAST 2-D DOA AND POLARIZATION ESTIMATION USING ARBITRARY CONFORMAL ANTENNA ARRAY

P. Yang<sup>1,\*</sup>, F. Yang<sup>1</sup>, Z. P. Nie<sup>1</sup>, H. J. Zhou<sup>2</sup>, B. Li<sup>3</sup>, and X. F. Tang<sup>3</sup>

<sup>1</sup>School of Electronic Engineering, University of Electronic Science and Technology of China (UESTC), Chengdu, China

<sup>2</sup>Institute of Applied Physics and Computational Mathematics, Beijing, China

<sup>3</sup>China Academy of Engineering Physics, Mianyang, China

**Abstract**—A fast and simple parameter estimation algorithm, joint azimuth angles, elevation angles and polarization parameters of incident sources for an arbitrary conformal array is proposed. Based on 2-D Discrete Fourier Transform (2-D DFT), the computational complexity can be reduced significantly compared with traditional 2-D space-search MUSIC or polynomial rooting (search-free) methods. The antenna elements can be mounted on arbitrary curved surfaces or platforms. Conformal array characteristics, such as directional radiation patterns of the elements and polarization are taken into consideration. Numerical simulations based on real-world conformal arrays are provided to demonstrate the performance of the proposed method.

### 1. INTRODUCTION

Direction-of-arrival (DOA) estimation techniques have been frequently used in many applications such as radar, sonar, astronomy and wireless communications [1–4]. Among these applications, most arrays are linear or planar structures with uniformly polarized antenna elements. Antenna arrays with diverse polarization have some inherent advantages over uniformly polarized arrays since they are capable of discriminating signals based on their polarization characteristics. For

---

*Received 7 July 2011, Accepted 4 November 2011, Scheduled 13 November 2011*

\* Corresponding author: Peng Yang (yangp001@tom.com).

example, they have been used in radar systems to improve clutter rejection, to discriminate between different types of targets and to reject main lobe interferences. Furthermore, polarization diversity can improve the robustness to channel fading in wireless communications.

In early work, DOA estimation using diversely polarized array was based on a multi-dimensional search procedure, such as MUSIC algorithm [5] and maximum likelihood (ML) algorithm [6, 7]. These methods suffer a high computational complexity. Hence, it is hard to use them in real time applications. In [8], a polynomial rooting based method for direction and polarization estimation using diversely polarized antennas was proposed. Compared with search based methods, the computational complexity of the polynomial rooting method (or search-free method) is reduced significantly. The limitations of [8] are that it can just estimate one dimensional angle (i.e., the antennas and sources are coplanar, in which case the elevation angle  $\theta = 90^\circ$ ), and all antenna elements are supposed to be omnidirectional. Recently, the work in [9] generalized [8] to arbitrary elevation angles, to directional antennas and to arbitrary antenna orientations. However, the procedure in [9] seems still complicated since estimated azimuth angles and elevation angles need to be paired. Goossens and Rogier [10] used phase-mode expansion for the induced voltages over the antenna elements in combination with the symmetry of the array to develop a computationally efficient method for DOA and polarization estimation. In his work, all electromagnetic effects including mutual coupling were taken into consider. But this method can just deal with DOAs with a fixed elevation angle. In [11], a novel blind DOA and polarization estimation method for polarization-sensitive uniform circular array was investigated. Based on generalized ESPRIT algorithm, better performance was achieved. But this method seems to be useful only for uniform circular array. Very recently, stemming from RARE (Rank Reduction Estimation) algorithm [12] and EADF (Effective Aperture Distribution Function) [13, 14] concept, Richter et al. proposed an very different method to estimate DOAs and polarization coefficients using arbitrary array configurations [15]. Later, this method had been extended in [16] and [17]. By constructing a nonlinear system of two bivariate polynomials and using the technique of Polynomial Root Intersection for Multidimensional Estimation (PRIME) [18], the problem can be solved by rooting procedure. The merit of [16] and [17] is that it can be used for arbitrary array configurations even for conformal arrays. Moreover, the estimated elevation and azimuth angles can be paired automatically, avoiding the complex pair procedure in [9]. However, solving the problem of two bivariate polynomials is not a easy thing, especially

when the orders of the polynomials become high.

We present a simple but fast method for 2-D DOA and polarization parameters estimation using conformal antenna arrays. Instead of constructing a Vandermonde structure for the cost function, in this paper, the 2-D DOAs can be obtained more efficiently by applying 2-D TDFT to the zeros padded coefficients, thus avoiding polynomial rooting. This paper is organized as follows. First, in Section 2, the signal model of arbitrary conformal array configurations with polarized antenna elements is introduced. In Section 3, we define a multivariate function then using 2-D DFT to solve this problem. In Section 4, the proposed method is verified by some numerical simulations based on real world conformal arrays. Finally, Section 5 concludes the paper.

## 2. SIGNAL MODEL

We begin by considering an arbitrary configuration polarimetric array with  $M$  antenna elements (Note that for 2-D DOA estimation, we need an array with 2-D configuration. 1-D linear array is not included in the “arbitrary configuration”). Each element is a dual polarized antenna composed by two orthogonal ports which can receive the horizontal and vertical components of the incident electromagnetic field independently. Assume  $P$  narrow band signals come from directions of  $(\theta_p, \phi_p)$ ,  $p = 1, 2, \dots, P$ . Where  $\theta$  is the elevation angle and  $\phi$  is the azimuth angle. The  $M \times 1$  output vector of the array at  $t$ th sample is given by

$$\mathbf{X}(\theta, \phi, \gamma, \eta, t) = \mathbf{F}(\theta, \phi) \cdot \mathbf{A}(\theta, \phi, \gamma, \eta) \mathbf{S}(t) + \mathbf{N}(t) \quad (1)$$

where  $\mathbf{F}(\theta, \phi) \in \mathbb{C}^{M \times P}$  is the active element pattern matrix. Its  $(m, p)$ th element represents the response of  $m$ th ( $m = 1, 2, \dots, M$ ) antenna element to  $p$ th signal comes from  $(\theta_p, \phi_p)$ . Note the active element pattern can be obtained by exciting an antenna with a unit voltage, while other antennas are terminated by matching impedance  $Z_0$  ( $Z_0 = 50 \Omega$ ). Usually, the active element pattern of each antenna is different because of the mutual coupling [19].

The matrix  $\mathbf{A}(\theta, \phi, \gamma, \eta) \in \mathbb{C}^{M \times P}$  is the steering matrix. Its  $p$ th column  $\mathbf{A}_p(\theta, \phi, \gamma, \eta) \in \mathbb{C}^{M \times 1}$  can be represented by

$$\mathbf{A}_p(\theta, \phi, \gamma, \eta) = \mathbf{V}_p(\theta, \phi) \mathbf{\Gamma}_p(\gamma, \eta) \cdot \mathbf{a}_p(\theta, \phi) \quad (2)$$

where the matrix  $\mathbf{V}_p(\theta, \phi) = [\mathbf{V}_h^p \ \mathbf{V}_v^p] \in \mathbb{C}^{M \times 2}$  and

$$\begin{aligned} \mathbf{V}_h^p &= -\mathbf{V}_x \sin \phi_p + \mathbf{V}_y \cos \phi_p \\ \mathbf{V}_v^p &= \mathbf{V}_x \cos \theta_p \cos \phi_p + \mathbf{V}_y \cos \theta_p \sin \phi_p - \mathbf{V}_z \sin \theta_p \end{aligned} \quad (3)$$

where  $\mathbf{V}_x \in \mathbb{C}^{M \times 1}$  are the voltages induced at the antennas output terminals by an incoming signal with a unit electric field polarized entirely along  $x$  direction. Similarly,  $\mathbf{V}_y$  and  $\mathbf{V}_z$  are the output voltages induced by signals with unit electric fields polarized along  $y$  and  $z$  directions, respectively. The polarization coefficient matrix  $\mathbf{\Gamma}_p(\gamma, \eta) \in \mathbb{C}^{2 \times 1}$  is defined as

$$\mathbf{\Gamma}_p = [\cos \gamma_p \quad \sin \gamma_p e^{j\eta_p}]^T \quad (4)$$

where  $\gamma$  and  $\eta$  define the signal's polarization angle and phase difference, respectively.  $(\cdot)^T$  denotes transpose.

$\mathbf{a}_p(\theta, \phi) \in \mathbb{C}^{M \times 1}$  represents the  $p$ th signal's steering vector. Its  $m$ th element is

$$a_m(\theta_p, \phi_p) = \exp [jk(x_m \sin \theta_p \cos \phi_p + y_m \sin \theta_p \sin \phi_p + z_m \cos \theta_p)] \quad (5)$$

where  $x_m$ ,  $y_m$  and  $z_m$  are the coordinates of the  $m$ th antenna and  $k = 2\pi/\lambda$  is the wave number.

Finally,  $\mathbf{S}(t) \in \mathbb{C}^{P \times 1}$  is the signal vector and  $\mathbf{N}(t) \in \mathbb{C}^{M \times 1}$  is the vector represents additive white noise. The problem here is how to use the finite receiving data  $\mathbf{X}$  in (1) to estimate the DOAs  $(\theta_p, \phi_p)$  and polarizations  $(\gamma_p, \eta_p)$ .

### 3. DOA AND POLARIZATION ESTIMATION BY 2-D DFT

In this section, 2-D DFT is applied for joint azimuth angle, elevation angle and polarization parameters estimation. We start by defining a new matrix that includes the information of signal DOAs and antenna polarizations as follows

$$\mathbf{B}(\theta, \phi, \gamma, \eta) = \mathbf{W}(\theta, \phi)\mathbf{\Gamma}(\gamma, \eta) \quad (6)$$

where

$$\mathbf{W}(\theta, \phi) = \text{diag}\{\mathbf{a}(\theta, \phi)\}\mathbf{V}(\theta, \phi) \quad (7)$$

According to classical MUSIC algorithm [1], we can construct a cost function as

$$D(\theta, \phi, \gamma, \eta) = \mathbf{B}^H \mathbf{G} \mathbf{G}^H \mathbf{B} = \mathbf{\Gamma}^H \mathbf{W}^H \mathbf{G} \mathbf{G}^H \mathbf{W} \mathbf{\Gamma} \quad (8)$$

where  $\mathbf{G} \in \mathbb{C}^{M \times (M-P)}$  is the noise subspace whose columns are the eigenvectors corresponding to the  $M - P$  smallest eigenvalues of the sample covariance matrix. From (8), it can be proved [8] that if  $\mathbf{W}$  is known, the minimum of  $D$  is obtained when  $\mathbf{\Gamma}$  is equal to the eigenvector corresponding to the smallest eigenvalue of the  $2 \times 2$  matrix

$$\mathbf{C}(\theta, \phi) = \mathbf{W}(\theta, \phi)^H \mathbf{G} \mathbf{G}^H \mathbf{W}(\theta, \phi) \quad (9)$$

Note that in Equation (9), the matrix  $\mathbf{W}(\theta, \phi)$  is dependent on the angles only. Hence, the DOA can be estimated first before the polarization parameters. In Reference [8], a root-MUSIC based method was proposed to solve Equation (9). However, it can only solve 1-D problem (the elevation angle is supposed to be fixed at  $90^\circ$ ). Moreover, it needs to root a polynomial with  $M$  order, the procedure of finding the roots becomes time-consuming if  $M$  is a very large number. To extend [8] to 2-D DOA estimation, and solve (9) efficiently, a 2-D DFT based technique [20], [21] is applied. The procedure is as follow:

First, we define the cost function as

$$f(\theta, \phi) = \det\{\mathbf{C}\} = \det\{\mathbf{W}^H \mathbf{G} \mathbf{G}^H \mathbf{W}\} \quad (10)$$

where  $\det\{\cdot\}$  denotes determinant. From (10) we found if  $(\theta, \phi)$  is the true DOA,  $f(\theta, \phi)$  will equal to zero. Since the function  $f(\theta, \phi)$  is a periodic function in  $\theta$  and  $\phi$ , it can be expanded using finite 2-D Fourier series

$$f(\theta, \phi) \approx \sum_{m=-L}^L \sum_{n=-K}^K F_{mn} e^{jm\theta} e^{jn\phi} \quad (11)$$

where the Fourier coefficient is

$$F_{mn} \approx \frac{1}{4\pi^2} \sum_{l=-L}^L \sum_{k=-K}^K f(l\Delta\theta, k\Delta\phi) e^{-jml\Delta\theta} e^{-jnk\Delta\phi} \quad (12)$$

where  $\Delta\theta = 2\pi/(2L + 1)$  and  $\Delta\phi = 2\pi/(2K + 1)$ .  $2L + 1$  and  $2K + 1$  are number of samples in  $\theta$  and  $\phi$  direction, respectively. The Fourier coefficient matrix  $\mathbf{F}_{co} \in \mathbb{C}^{(2L+1) \times (2K+1)}$  can be obtained quickly by using 2-D FFT. After the Fourier coefficients are obtained, to improve the resolution, we can use zeros padding, i.e.,

$$\hat{F}_{mn} = \begin{cases} F_{mn}, & \text{for } |m| < 2L+1, \quad \text{and } |n| < 2K+1 \\ 0, & \text{for } 2L+1 < |m| < L_0, \quad \text{and } 2K+1 < |n| < K_0 \end{cases} \quad (13)$$

Usually, we select  $L_0 \gg 2L + 1$  and  $K_0 \gg 2K + 1$ . The new cost function  $\hat{f}(\theta, \phi)$  of every grid can be calculated efficiently by applying 2-D IFFT to the zeros padded Fourier coefficient matrix  $\hat{\mathbf{F}}_{co} \in \mathbb{C}^{L_0 \times K_0}$ . Recalling that the true DOAs will make  $f(\theta, \phi)$  close to zero. Hence, the estimated  $P$  pair of angles  $(\hat{\theta}, \hat{\phi})$  can be easily obtained from the  $P$  maximum peaks of the null-spectrum  $1/\hat{f}(\theta, \phi)$ .

Note that the computational complexity of the traditional 2-D space-search MUSIC algorithm and the 2-D DFT based method are totally different. For traditional 2-D space-search MUSIC algorithm, to get acceptable accuracy, we need divide the interested area into

very dense grids. For example, if the interested area is  $\theta \in [0^\circ, 90^\circ]$ ,  $\phi \in [-45^\circ, 45^\circ]$  and the unit grid is  $0.1^\circ \times 0.1^\circ$ , we need calculate  $901 \times 901 = 811801$  times the matrix-vector product  $\mathbf{W}^H \mathbf{G}$  in (10). However, in the 2-D DFT method, only  $(2L + 1) \times (2K + 1)$  matrix-vector products in (10) need to be calculated (In our simulation,  $L = K = 34$ ,  $(2L + 1) \times (2K + 1) = 69 \times 69 = 4761$ ). For other grids, we use zero-padding directly. Hence, the decrease of computational complexity is considerable. Also, this method has a lower complexity than the 2-D polynomial rooting method. For example, in references [16] and [17], to estimate the 2-D DOAs, more time is needed to solve the high order bivariate nonlinear polynomials. Since rooting a bivariate nonlinear polynomial is computationally very intensive and 2-D FFT/IFFT technique for real time implementation is readily available, the 2-D DFT based approach appears to be competitive.

Once the estimated angles  $(\hat{\theta}_p, \hat{\phi}_p)$  of the  $P$  signals are obtained, we can calculate the eigenvectors and eigenvalues of matrix  $\hat{\mathbf{C}}$  in (9). Let  $\mathbf{u}_p \in \mathbb{C}^{2 \times 1}$  be the eigenvector corresponding to the smallest eigenvalue of  $\hat{\mathbf{C}}$ , the estimated polarization coefficients can be obtained by [16]

$$\begin{cases} \hat{\mathbf{v}}_p = \mathbf{u}_p \mathbf{u}_p^* (1) / |\mathbf{u}_p (1)| \\ \hat{\gamma}_p = \arccos(\hat{\mathbf{v}}_p (1)) \\ \hat{\eta}_p = \angle \hat{\mathbf{v}}_p (2) \end{cases} \quad (14)$$

To summarize, the proposed fast 2-D DFT based algorithm for arbitrary conformal arrays can be accomplished via the following steps:

1. Form the received data covariance matrix and perform eigenvalue decomposition to obtain the noise subspace matrix  $\mathbf{G}$ .
2. Calculate the cost function  $f(\theta, \phi)$  in (10) using the finite  $(2L + 1) \times (2K + 1)$  samples.
3. Apply 2-D FFT to calculate the Fourier coefficient matrix  $\mathbf{F}_{co} \in \mathbb{C}^{(2L+1) \times (2K+1)}$ .
4. Use zeros padding to form a large matrix  $\hat{\mathbf{F}}_{co} \in \mathbb{C}^{L_0 \times K_0}$ . Note that  $L_0 \gg 2L + 1$  and  $K_0 \gg 2K + 1$ .
5. Apply 2-D IFFT to get a new cost function  $\hat{f}(\theta, \phi)$ . The estimated DOAs can be found from the null-spectrum  $1/\hat{f}(\theta, \phi)$ .
6. Perform eigenvalue decomposition to matrix  $\hat{\mathbf{C}}$  and use Equation (14) to estimate the polarization coefficients.

#### 4. NUMERICAL SIMULATIONS

In this section, two numerical examples are provided to evaluate the performance of the proposed method. The first example is a uniform 5 by 5 cylindrical conformal array shown in Figure 1. The antennas are mounted on a metallic cylinder with the height of  $4\lambda$  and radius of  $1.28\lambda$ . Here  $\lambda$  is the antenna operating frequency in free space. The distance of adjacent element is equally spaced at approximately  $0.5\lambda$  in  $\theta$  and  $\phi$ . The antennas are dual polarized microstrip antennas and

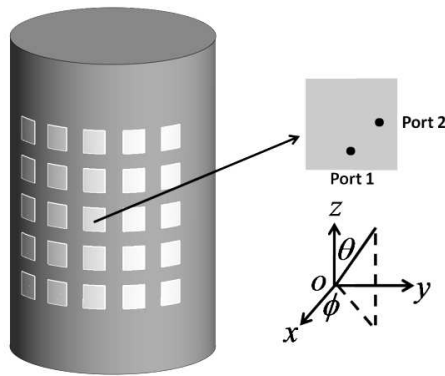


**Figure 1.** Cylindrical conformal array with 5 by 5 dual polarized microstrip antenna elements.

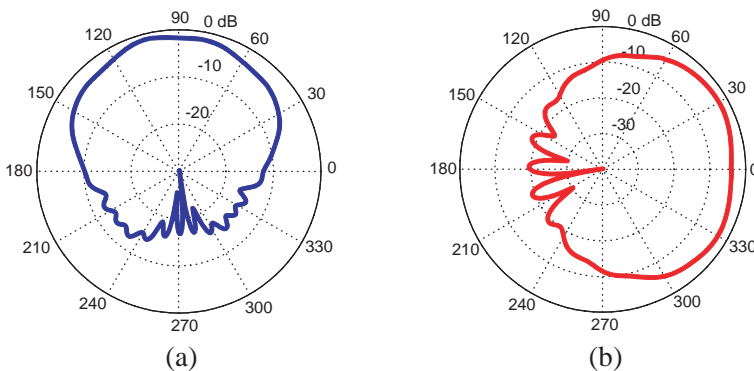
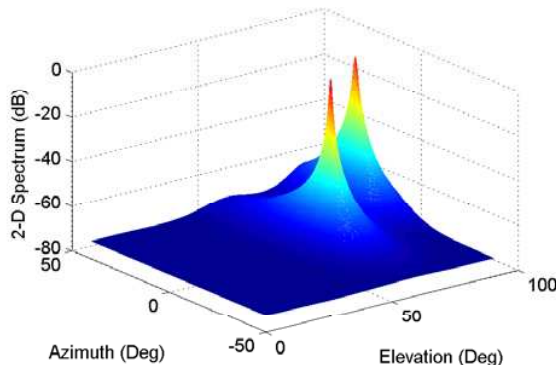


**Figure 2.** Radiation patterns ( $E$ -plane) of the antenna in the middle of the array. (a) Vertical polarized ( $xoz$  plane). (b) Horizontal polarized ( $xoy$  plane).

each antenna has two ports to receive two orthogonal components. The active radiation patterns were obtained by using full wave numerical code based on Method of Moment (MOM). For each antenna, both the 3-D active radiation patterns of two orthogonal ports were calculated. The E-pattern of the horizontal ( $\theta = 90^\circ$ ) and vertical ( $\phi = 0^\circ$ ) slices of the antenna in the middle of the array were plotted in Figure 2(a) and Figure 2(b), respectively. It needs to be noted that each antenna has a unique radiation pattern because their different locations in the array and the effects of mutual coupling.

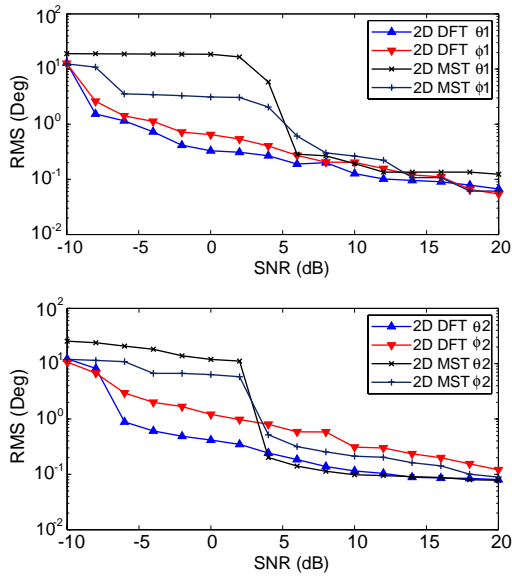
Assume two uncorrelated narrow band signals come from ( $\theta_1 = 60^\circ, \phi_1 = 0^\circ$ ) and ( $\theta_2 = 85^\circ, \phi_2 = 20^\circ$ ). One signal is elliptical polarized and another one is linearly polarized. The polarization coefficients are ( $\gamma_1 = 30^\circ, \eta_1 = 10^\circ$ ) and ( $\gamma_2 = 45^\circ, \eta_2 = 0^\circ$ ), respectively. The snapshots is fixed to 128. In this simulation, the sample points in  $\theta$  and  $\phi$  direction are  $2L + 1 = 2K + 1 = 69$ . The dimension of the zeros padded Fourier coefficient matrix  $\hat{\mathbf{F}}_{co}$  is  $L_0 \times K_0 = 2048 \times 2048$ . The noise is additive Gaussian white noise. 100 Monte-Carlo experiments are carried out. The 2-D manifold separation technique (2-D MST) proposed in [16] is used for comparison.

Figure 3 shows the 2-D spectrum of the null-spectrum function  $1/\hat{f}(\theta, \phi)$ . The SNR of two signals are 20 dB. Similar to traditional 2-D space-search MUSIC algorithm, two sharp peaks are observed. However, just as aforementioned, the ways to obtain this spectrum are totally different. Figure 4 is the RMS of the estimated DOAs with different SNR of the two methods. It can be seen that the 2-D DFT based method has a higher performance than the 2-D MST based method at low SNR level. When  $\text{SNR} > 0$  dB, the RMS of two



**Figure 3.** 2-D spectrum of the null-spectrum function  $1/\hat{f}(\theta, \phi)$  of cylindrical conformal array (SNR=20 dB).





**Figure 4.** RMS of two estimated DOAs with different SNR on cylindrical conformal array. ( $\theta_1 = 60^\circ$ ,  $\phi_1 = 0^\circ$ ) and ( $\theta_2 = 85^\circ$ ,  $\phi_2 = 20^\circ$ ).

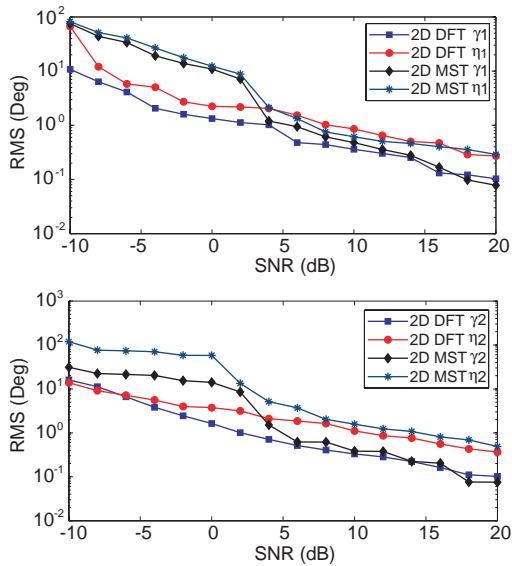


**Figure 5.** RMS of two estimated polarization parameters with different SNR on cylindrical conformal array. ( $\gamma_1 = 30^\circ$ ,  $\eta_1 = 10^\circ$ ) and ( $\gamma_2 = 45^\circ$ ,  $\eta_2 = 0^\circ$ ).

signals are both below one degree by using the 2-D DFT method. The estimated performances of elevation angles are better than azimuth angles because the array-aperture in the elevation angle is bigger than the array-aperture in the azimuth angle. With the SNR increases (SNR > 5 dB), the 2-D MST has a similar performance compared to 2-

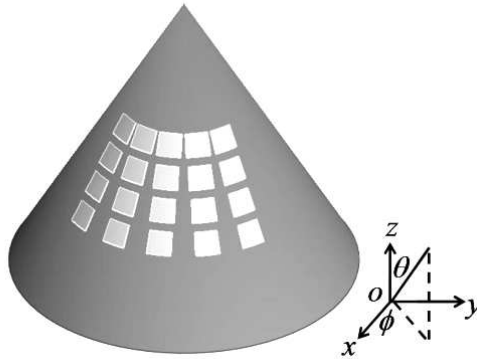


**Figure 6.** Conical conformal array with 5 by 4 dual polarized microstrip antenna elements.

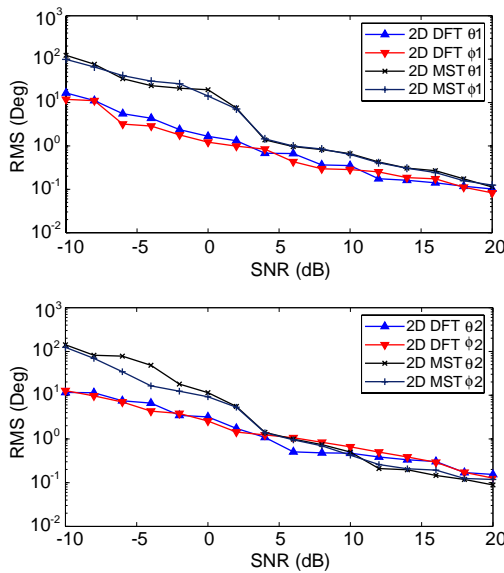


**Figure 7.** RMS of two estimated DOAs with different SNR on conical conformal array. ( $\theta_1 = 60^\circ$ ,  $\phi_1 = 0^\circ$ ) and ( $\theta_2 = 85^\circ$ ,  $\phi_2 = 20^\circ$ ).

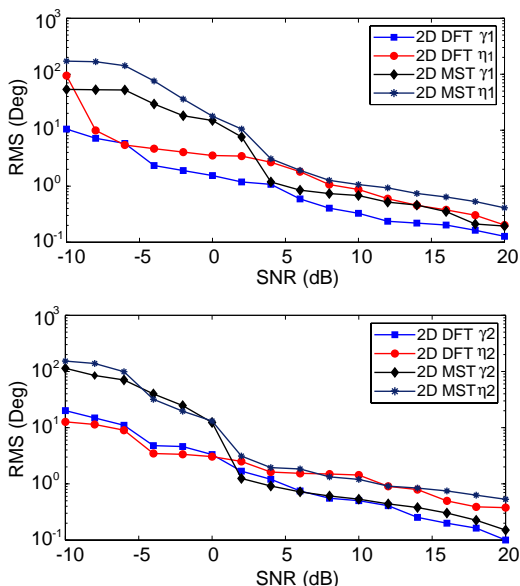


**Figure 8.** RMS of two estimated polarization parameters with different SNR on conical conformal array. ( $\gamma_1 = 30^\circ$ ,  $\eta_1 = 10^\circ$ ) and ( $\gamma_2 = 45^\circ$ ,  $\eta_2 = 0^\circ$ ).

D DFT method. The RMS of two estimated polarization parameters with different SNR are plotted in Figure 5. Similarly, compared to 2-D MST, we find that the 2-D DFT method has a better performance at low SNR level but a same performance at high SNR level.

To verify that this method can be applied for arbitrary arrays, in the second example, a 5 by 4 conical conformal array is used for test. The cone shown in Figure 6 has a base with a radius about  $3.7\lambda$  and semi-cone angle of  $30^\circ$ . The parameters of the signals are the same as the first example. The estimated performances of DOAs and polarization coefficients are shown in Figure 7 and Figure 8, respectively. Again, good results are obtained by using 2-D DFT method.

Table 1 gives the time consumed by the two methods (100 simulations time). In 2-D MST method, there is an off-line pretreatment procedure to construct the calibration matrix [16]. The 2-D MST costs about 5 hours to do 100 simulations. The 2-D DFT method, however, costs only 80 seconds. The enhancement of the speed is considerable.

**Table 1.** Time consuming of the two methods (100 simulations time, AMD 3.0 GHz, Windows XP 32 bit, 3 GB memory, Matlab 7.10).

	Pretreatment time	Calculation time	Total time
2D DFT (cylindrical array)	--	80.3 s	80.3 s
2D MST (cylindrical array)	7.8 s	20713 s	20720.8 s
2D DFT (conical array)	--	73.5 s	73.5 s
2D MST (conical array)	6.3 s	19871 s	19877.3 s

## 5. CONCLUSIONS

In this paper, we present a fast method for 2-D DOA and polarization estimation for arbitrary conformal arrays. The algorithm uses 2-D DFT to calculate the null-spectrum function, and it does not require an explicit space-search or polynomial roots finding procedure. The performance of this method is evaluated by numerical simulations on different conformal arrays. Theoretical analysis and simulation results verify that this method combines accuracy with low computational requirements.

## ACKNOWLEDGMENT

This work is supported by NASF (No. 10876007 and No. 11176007) and NSTMP (No. 2010ZX03007-001-04).

## REFERENCES

1. Liang, J. and D. Liu, "Two L-shaped array-based 2-d DOAs estimation in the presence of mutual coupling," *Progress In Electromagnetics Research*, Vol. 112, 273–298, 2011.
2. Yang, P., F. Yang, and Z.-P. Nie, "DOA estimation with sub-array divided technique and interpolated esprit algorithm on a cylindrical conformal array antenna," *Progress In Electromagnetics Research*, Vol. 103, 201–216, 2010.

3. Mukhopadhyay, M., B. K. Sarkar, and A. Chakraborty, "Augmentation of anti-jam GPS system using smart antenna with a simple DOA estimation algorithm," *Progress In Electromagnetics Research*, Vol. 67, 231–249, 2007.
4. Tu, T.-C., C.-M. Li, and C.-C. Chiu, "The performance of polarization diversity schemes in outdoor micro cells," *Progress In Electromagnetics Research*, Vol. 55, 175–188, 2005.
5. Schmitz, R. O., "Multiple emitter location and signal parameter estimation," *IEEE Trans. Antennas Propag.*, Vol. 34, No. 3, 276–280, Mar. 1986.
6. Siskind, I. and M. Wax, "Maximum likelihood localization of diversely polarized sources by simulated annealing," *IEEE Trans. Antennas Propag.*, Vol. 38, No. 7, 1111–1114, July 1990.
7. Lizzi, L., F. Viani, M. Benedetti, P. Rocca, and A. Massa, "The m-DSO-esprit method for maximum likelihood DOA estimation," *Progress In Electromagnetics Research*, Vol. 80, 477–497, 2008.
8. Weiss, A. J. and B. Friedlander, "Direction finding for diversely polarized signals using polynomial rooting," *IEEE Trans. Signal Process.*, Vol. 41, No. 5, 1893–2021, May 1993.
9. Wong, K. T., L. S. Li, and M. D. Zoltowski, "Root-MUSIC-based direction-finding and polarization estimation using diversely polarized possibly collocated antennas," *IEEE Antennas Wireless Propag. Lett.*, Vol. 3, 129–132, 2004.
10. Goossens, R. and H. Rogier, "Estimation of direction-of-arrival and polarization with diversely polarized antennas in a circular symmetry incorporating mutual coupling effects," *Proc. EuCAP*, Nice, France, 2006.
11. Zhang, X., Y. Shi, and D. Xu, "Novel blind joint direction of arrival and polarization estimation for polarization-sensitive uniform circular array," *Progress In Electromagnetics Research*, Vol. 86, 19–37, 2008.
12. Pesavento, M., C. F. Mecklenbrauker, and J. F. Bohme, "Multidimensional rank reduction estimator for parametric MIMO channel models," *European Journal on Applied Signal Processing*, No. 9, 1354–1363, 2004.
13. Richter, A., "Estimation of radio channel parameters: Models and algorithms," Ph.D. Thesis Dissertation, TU Ilmenau, 2005.
14. Belloni, F., A. Richter, and V. Koivunen, "DoA estimation via manifold separation for arbitrary array structures," *IEEE Trans. Signal Process.*, Vol. 55, No. 10, 4800–4810, Oct. 2007.
15. Richter, A., F. Belloni, and V. Koivunen, "DoA and polarization

- estimation using arbitrary polarimetric array configurations," *IEEE Workshop Sensor Array and Multichannel Processing (SAM)*, 55–59, 2006.
16. Costa, M., A. Richter, and V. Koivunen, "Azimuth, elevation and polarization estimation for arbitrary polarimetric array configurations," *IEEE Workshop on Statistical Signal Process.*, 261–264, 2009.
  17. Costa, M., A. Richter, and V. Koivunen, "Low complexity azimuth and elevation estimation for arbitrary array configurations," *IEEE Intern. Conf. Acoust. Speech Signal Process.*, 2185–2188, 2009.
  18. Hatke, G. F. and K. W. Forsythe, "A class of polynomial rooting algorithms for joint azimuth/elevation estimation using multidimensional arrays," *Asilomar Conference on Signals, Systems and Computers*, Vol. 1, 694–699, 1995.
  19. Goossens, R. and H. Rogier, "Optimal beam forming in the presence of mutual coupling," *Proc. Commun. Veh. Technol. Symp.*, 13–18, 2006.
  20. Rubsamen, M. and A. B. Gershman, "Direction of arrival estimation for nonuniform sensor arrays: From manifold separation to Fourier domain music methods," *IEEE Trans. Signal Process.*, Vol. 57, No. 2, 588–599, 2009.
  21. Babu, K. V. S., "A fast algorithm for adaptive estimation of root-MUSIC polynomial coefficients," *Proc. Int. Conf. Acoustics, Speech, Signal Processing (ICASSP)*, 2229–2232, Toronto, ON, Canada, May 1991.